Optimal combination and reference functions of signal-to-noise measurements for GNSS multipath detection

Peter Špánik[1], Luis García-Asenjo[2] and Sergio Baselga[3*]

[1]Slovak University of Technology in Bratislava, Faculty of Civil Engineering, Department of Theoretical Geodesy, Radlinského 11, 810 05 Bratislava, Slovakia
[2,3*]Universitat Politècnica de València, Cartographic Engineering, Geodesy and Photogrammetry Department, Camino de Vera s/n, 46022 Valencia, Spain

E-mails: [1]peter.spanik@stuba.sk, [2]lugarcia@cgf.upv.es, [3*]serbamo@cgf.upv.es ([*]Corresponding author)

Received xxxxxx
Accepted for publication xxxxxx
Published xxxxxx

Abstract

Multipath is the most limiting factor in many GNSS positioning applications, where it inevitably degrades the attainable precision. Among the different proposals to identify observations affected by multipath, Strode and Groves have recently proposed a method based on the comparison of GPS signal-to-noise (SNR) actual measurements with suitable reference functions previously computed in a low-multipath environment. We have found significant issues with its application to our particular GNSS experiments, however. In particular, we discuss whether the reference functions that are needed to be computed for low-multipath environments after tedious and time consuming field campaigns can be used for a future occasion, or not, as well as the possibility of applying the method to other GNSS global constellations (Galileo and GLONASS). Additionally, we elaborate on an alternative idea consisting in the use of the best combination of SNR measurements for the different signals in the different constellations in order to obtain a multipath estimator that is unbiased, universal and performs better than the use of reference functions.

Keywords: multipath, multi-constellation, SNR

1. Introduction

Multipath is the most limiting factor in many positioning applications ranging from submillimetric GNSS distance determination to kinematic applications in urban environments [1-4]. Even taking all possible precautions and using state-of-the-art GNSS components, its undesirable occurrence is ordinary and it inevitably degrades the attainable precision. The correct identification of the presence of multipath in a particular signal of any of the existing GNSS constellations is a challenge at present. Succeeding in this task would represent an undeniable step forward for many positioning applications.

Among the vast number of proposals for detecting multipath, e.g. [5-13], Strode and Groves recently proposed a combination of GPS signal-to-noise (SNR) measurements showing a large degree of success in the identification of observations affected by multipath [14]. The method is appealing and easy to implement, since besides the SNR values recorded by the receiver and included in the Receiver INdependent EXchange (RINEX) files no additional data are needed for the analysis. It is applicable in post-processing as

well as in real time provided the required calibration has been previously done.

Several issues in applying the method to our particular experiments were found, however. To start with, it needs the additional acquisition of data in a low-multipath calibration environment that is to be subtracted from the data from the actual environment for the computation of the multipath estimator. Whether or not the reference functions computed from these low-multipath SNR observations can be used for a future occasion (in the same place or even different place), thus alleviating the observation phase, or not, is something that has not been carefully studied yet. Nor has the possibility of application to other GNSS global constellations (Galileo, GLONASS and BeiDou). The proponents' idea of constructing the reference function by fitting a third-order polynomial to the observations is also questionable, as is the computation of the significance values for the thresholds proposed, since the underlying statistical distribution of the estimator has not been established. In addition, the estimator is computed for one satellite only, whereas the case of double-differenced observations (two satellites and two receivers), which is standard in many geodetic applications, remains unexplored.

In the present contribution we analyze the estimator proposed by Strode and Groves [14] for the different signals in three GNSS constellations: GPS, Galileo and GLONASS. One of the most striking results we obtain is the remarkably different shape of the reference functions for the different constellations: in the case of two frequencies, for GPS with the shape of a straight line with moderate slope, for Galileo being a horizontal straight line (almost at zero), and with a satellite-dependent shape for GLONASS suggesting a possible linear relationship in terms of carrier wave frequency. The possibilities of a universal definition and use of reference functions for the different constellations are also addressed, as is the disquieting lack of consistency in the detection of multipath that we occasionally found in our experiments for cases where the receiver-satellite-environment geometry suggests the presence of severe multipath.

In addition to the estimator presented by Strode and Groves [14], we also elaborate on an alternative idea consisting in the use of the best combination of SNR measurements for the different signals in the different constellations in order to obtain a multipath estimator that is unbiased (from zero), universal (any time, any place, same equipment) and performs better than the use of reference functions. For both approaches, we also analyze the possible benefit of correcting raw SNR values by considering the user's antenna gain.

Finally, we compare the practical performances of both methods based on the use of SNR measurements (the method using reference functions and the one using the optimal combination of SNR values) as well as other comparably simpler-to-use methods (e.g. decision trees obtained from machine learning algorithms).

2. Methods

In this section we will describe the two main methods used for this research: the method based on the use of reference functions, i.e. the approach presented by Strode and Groves [14], which has already been used in other works (e.g. [15]), and the novel method presented in this contribution based on the optimal combination of SNR values. For the sake of comparison we also present and then use a considerably simpler method based on a decision tree built from machine learning algorithms.

2.1 Method based on the reference function

The method presented by Strode and Groves [14] is motivated by the interaction between reflected and direct signals and its corresponding impact on observed SNR values. According to [16,17] the effect of the reflected signal has an impact on the resulting signal amplitude, which can be approximated by corresponding SNR value as

$$SNR_i^2 \approx A_{c(i)}^2 = A_{d(i)}^2 + A_{r(i)}^2 + 2A_{d(i)}\,A_{r(i)} \cos \Delta\Phi_{d,r(i)} \quad (1)$$

where A_c represents amplitude of the composite signal (which is tracked by the receiver), A_d is the amplitude of the direct signal, A_r is the amplitude of the reflected signal and $\Delta\Phi_{d,r}$ represents the phase shift between direct and reflected signal (sometimes also denoted as relative phase). Subscript i represents the index for the different carrier wavelengths of the used signal. The phase shift can be modelled as

$$\Delta\Phi_{d,r(i)} = \frac{\Delta d}{\lambda_i} \cdot 2\pi \quad (2)$$

where Δd is the path delay and λ_i is the signal wavelength. The path delay Δd is given for a time instant and it is only affected by the geometry of reflection in terms of the actual position of the satellite and objects in the vicinity of the antenna. By contrast, the phase shift value $\Delta\Phi_{d,r}$ varies according to the particular carrier wavelenght; therefore, different impacts on the SNR values in Eq. (1) are expected.

The fact that the presence of multipath on signal propagation has a different impact on observed SNR values for different carrier frequencies was used in [14] to propose a test statistic S from a set of SNR values and compare it with a threshold that marks the limit of the system's normal performance. The formula for computing the test statistic S is

$$S = \sqrt{\left(S_1 - S_2 - \Delta\hat{C}_{12}(\theta)\right)^2 + \left(S_1 - S_5 - \Delta\hat{C}_{15}(\theta)\right)^2} \quad (3)$$

where S_1, S_2, S_5 are measured SNR values in dbHz for the corresponding frequencies (originally proposed with GPS L_1, L_2 and L_5) and $\Delta\hat{C}_{12}$, $\Delta\hat{C}_{15}$ are reference functions which are dependent on satellite elevation θ. The computation of the test statistic S can be simplified to a two-frequency form by simply removing the second term under square root in Eq. (3). However, the two-frequency alternative may be more susceptible to incorrect multipath identification than the three-frequency version.

2.1.1 Reference functions. $\Delta\hat{C}_{12}$, $\Delta\hat{C}_{15}$ are estimated by means of a third-order polynomial fit of the SNR values differences $S_1 - S_2$ and $S_1 - S_5$. The fit is made against satellite elevation angle θ (independent variable) for data gathered in a low-multipath environment. They are taken as reference for comparison with current SNR values according to Eq. (3). In the original paper [14] data from only three GPS block II-F satellites (namely PRN 24, 25 and 27) were used in the analysis, because they were the only GPS satellites transmitting signals on three distinct frequencies at the time. At present, with many more satellites transmitting on three frequencies in GPS and the other constellations, we could use significantly more satellites. We have observed, however, that the shape of the reference functions for different constellations is substantially different. Even within a constellation we can appreciate some variations among its satellites although the possibility to model SNR differences on two frequencies for all satellites within a constellation using a single universal function is also discussed.

2.1.2 Multipath detection threshold. The threshold for multipath detection is estimated using detection statistic values S from Eq. (3) as an elevation dependent function

$$T(\theta) = \hat{S}(\theta) + t \cdot \hat{\sigma}_S \tag{4}$$

where the first part of the threshold $\hat{S}(\theta)$ is obtained by fitting a third-order polynomial to S values from data gathered in a low-multipath environment. The second term in the threshold function is a $t \approx 1$, 2 and 3-fold multiplication of fit standard deviation $\hat{\sigma}_S$ value. These three t-levels of threshold serve as multipath severity assessment. The idea of forming the threshold this way may be questionable inasmuch as the probabilities shall be understood to be different than the usual 68%, 95% and 99% corresponding to t = 1, 2 and 3 when the underlying distribution is the Normal distribution. This is clearly not the case, because detection statistic S values can be only positive and thus the resulting distribution is only one-sided (not two sided as the Normal distribution). The Normality of the raw SNR values may also be questionable.

2.2 Method based on the optimal combination

As an alternative approach to the comparison of the SNR actual differences with respect to their expected values as determined in a low-multipath environment (reference functions), we present now a new method based on the optimal combination of SNR measurements to obtain a multipath estimator whose value indicates the absence or presence of multipath. We propose the following estimator

$$S^* = S_1 + \alpha S_2 + \beta S_5 + \gamma cos(\theta) \tag{5}$$

where S_1, S_2 and S_5 denote the SNR measured values in dbHz for the corresponding frequencies (e.g. L_1, L_2 and L_5 in GPS) and θ denotes the elevation angle. It is understood that SNR values, as well as the elevation angle, are station-to-receiver dependent; therefore, subscripts and superscripts will not be used for the sake of clarity. α, β and γ are constants to be determined so that the resulting estimator S^* is close to zero for a low-multipath environment and significantly different from zero (e.g. three times its standard deviation or more) in the presence of multipath.

To determine α, β and γ we solve the least-squares system of equations of the type Eq. (5) for the different SNR measurements taken in a low-multipath environment. We will then use these values along with Eq. (5) for the detection of possible multipath in other environments. Similarly to the method based on reference functions we use the t-sigma rule for detection threshold understanding that the corresponding probabilities, irrespective of the underlying statistical distribution, can be bound by Chebyshev's inequality as

$$probability \geq 1 - \frac{1}{t^2} \tag{6}$$

This means a probability of at least 89% for t = 3 no matter the type of the underlying distribution.

At any rate, the statistical distribution of the S^* estimator will be shown to resemble the Normal distribution much more than the S estimator (for example, being significantly symmetrical around zero).

2.3 Method based on decision trees

Simple methods have been devised for quickly evaluating whether an observation is line-of-sight or not. These methods are quick to compute and easy to implement, as their intended applications are to real-time urban navigation. The simplest of them decides on the basis of signal strength only, while more elaborate proposals may be obtained by machine learning techniques, such as the decision tree in [18], which takes into account SNR, elevation and pseudorange residuals.

While non-line-of-sight reception and multipath are distinct concepts (for instance, a signal only received via reflection has no multipath) it is worth comparing the results

of non-line-of-sight detection with those of multipath detection. Ultimately, all observations flagged as non-line-of-sight will be excluded from the final adjustment.

3. Experiments

During the night of April 26-27, 2018, 8 hours of GNSS (GPS, Galileo and GLONASS) data were collected at 1 Hz rate using Trimble 5800 receivers in three different locations of the Universitat Politècnica de València campus (Spain), Figs. 1-3: one in the center of the field of an athletics track, which we call *Field*, Fig. 4, which was expected to be a station considerably free of multipath effects due to the absence of nearby constructions and potentially reflecting surfaces, other just next to the track near some buildings, called *Track*, Fig. 5, which was expected to have some observations clearly affected by multipath, and a third one on the roof of a nearby building, called *Roof*, Fig. 6, with a clear open sky but potentially affected by multipath due to reflections on nearby objects.

Figure 1. General 3D view of the *Field*, *Track* and *Roof* stations over a Google Earth view (© 2015 Google Inc., used with permission. Google and the Google logo are registered trademarks of Google Inc.).

Figure 2. Top view of the *Field*, *Track* and *Roof* stations over a Google Earth view (© 2015 Google Inc., used with permission. Google and the Google logo are registered trademarks of Google Inc.).

Figure 3. 3D view of the *Field*, *Track* and *Roof* stations over a Google Earth view (© 2015 Google Inc., used with permission. Google and the Google logo are registered trademarks of Google Inc.).

Figure 4. Detail view of *Field* station.

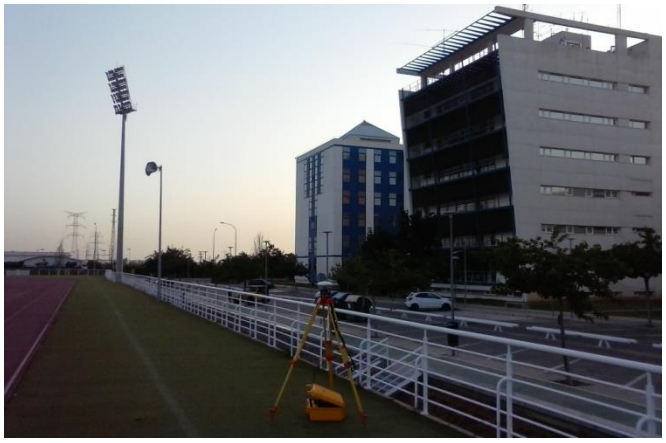

Figure 5. Detail view of *Track* station.

Figure 6. Detail view of *Roof* station.

4. Results and discussion

As noted previously in section 2 the method originally proposed for multipath detection using SNR reference functions can be improved in several ways.

4.1 Shape of reference functions for different GNSS constellations

For the reference functions method it is crucial to know what is the coincidence between the shape of polynomial fits for each satellite compared to the common fit estimated for all satellites together. Fig. 7 shows the reference functions of SNR differences at two different frequencies for all GNSS satellites tracked in the experiment (GPS, GLONASS and Galileo). We can see that the coincidence between common reference function and individual reference functions for the case of GPS is on good level. Based on this we can assume that a universal reference function can be used to model SNR differences. We can see that the universal function strongly depends on elevation angle, it varies approximatelly 12 dBHz in the given elevation range with smaller SNR differences at higher elevation.

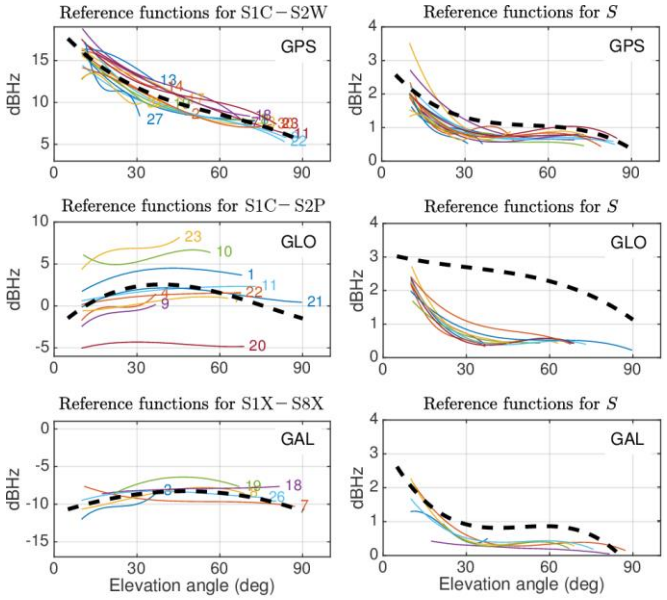

Figure 7. Left panels: reference functions $\Delta\hat{C}_{12}(\theta)$ estimated at site *Field* for all tracked GNSS systems for individual satellites alone (color lines with satellite numbers) and for all satellites together (bold black dashed line). Right panels: reference functions $\hat{S}(\theta)$ which fit statistics *S* values.

In case of GLONASS satellites there are visible offsets between individual reference functions. It is caused by large differences in the received signal powers for different frequencies. For satellites R04, R09 and R20 the signal strength S2P is even stronger than S1C (reference functions have negative values), which should not occur based on [19]. We know that the receiving signal strength is also strongly affected by the receiving antenna's gain pattern. However this effect should have more or less equal impact on all satellites, so this explanation seems not enough. Based on the observed inconsistency among the individual reference functions for GLONASS satellites we decided not to use the universal reference function for modelling SNR differences, so that in the following analysis we use individual reference functions for each satellite instead.

In the case of Galileo we observed that the consistency of individual reference functions is fairly good, thus the utility of a universal reference function. We can see that there is only a low dependency of reference functions according to elevation angle. We can also see significant negative values of reference values because signal strength on E5a+b carrier (S8X) is much stronger than on E1 carrier (S1X).

Reference functions which fit statistics *S* values are shown on the right panels of Fig. 7. We can see that these common reference functions fit the individual ones considerably well for the cases of GPS and Galileo. The values of these functions are then used for computation of threshold by Eq. (4). In the case of GLONASS satellites, the overall fit by $\hat{S}(\theta)$ is very poor because of the offsets present in reference functions $\Delta\hat{C}_{12}(\theta)$. For the threshold computation

we have used individual reference functions instead of one universal function.

4.2 Effect of antenna gain patterns

It is well known that observed SNR values are elevation dependent. The main reason for this elevation dependency is the receiving antenna gain pattern, which simply represents the sensitivity of the GNSS antenna to the incoming signal. Generally, GNSS antennas are build to have high gains for signals coming from above horizon (up to +5 dBi) and low gains for signals coming below horizon (-6 dBi and less) as we can see in Fig 8.

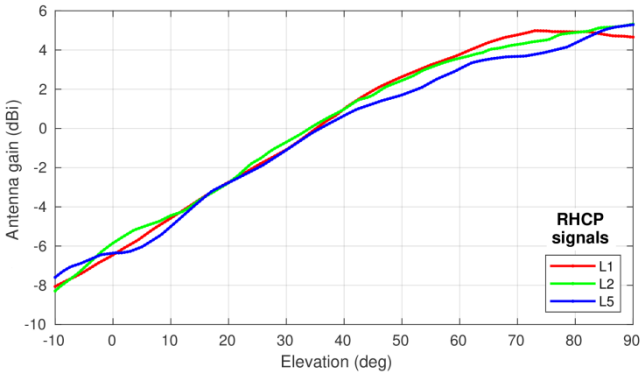

Figure 8. Antenna gain pattern of combined Trimble 5800 (R8 Model 3) GNSS receiver (personal communication with Trimble support via Geotronics, s.r.o) for right-hand circularly polarized (RHCP) signals for GPS L_1, L_2 and L_5 carriers.

After correcting antenna gains no significant differences were found, however, for the reference functions, threshold values and test statistic S values.

4.3 Optimal combination, S^* estimator

Regarding the approach using the optimal combination of SNR measurements, estimator S^*, Eq. (5), the SNR observations measured in the *Field* location are selected to determine the optimal combination. We also want to test whether the use of two frequencies (L_1 and L_2 for the case of GPS), i.e. $\beta = 0$ in Eq. (5), also provides an acceptable estimator, as well as the more simplified, naive approach of assigning -1 to both α and γ (in addition to $\beta = 0$). Fig. 9 shows the resulting values for satellite G9, which is here very convenient due to its trajectory in the sky as observed from *Field* location.

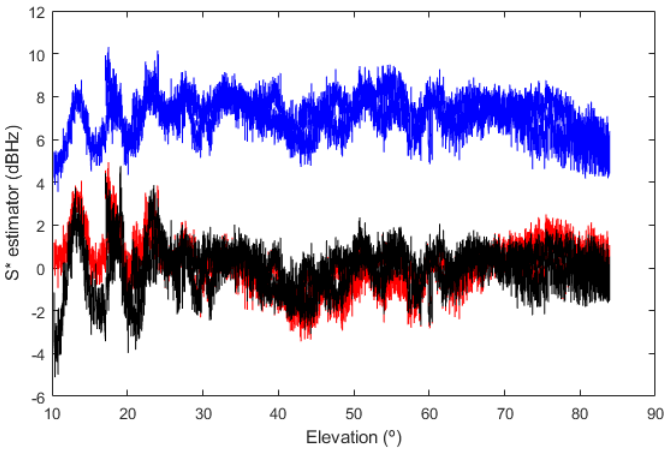

Figure 9. *Field* location. Values for different types of the S^* estimator, Eq. (5) in terms of the elevation angle (θ): in black the complete version $S^* = S_1 - 0.5386S_2 - 0.5074S_5 - 1.8733\cos\theta$, in red the two-frequency version $S^* = S_1 - 1.0954S_2 - 8.0239\cos\theta$, in blue the simplified two-frequency version $S^* = S_1 - S_2 - \cos\theta$.

As it can be seen the simplified two-frequency version $(\alpha,\beta,\gamma) = (-1,0,-1)$ does not yield the desired result and can be discarded as a feasible multipath detector. By contrast, we obtain reasonable and acceptable results both for the two-frequency and three frequency estimators, that is, some multipath for the lowest elevations, and no significantly high values (above 2) for higher elevations. We observe, as expected, that the S^* estimator takes on values around zero, especially for the not-too-low elevations inevitably affected by some multipath (we obtain a mean value of $\mu = 0.0024$ and a standard deviation of $\sigma = 1.0400$ for the complete version of the S^* estimator).

If we perform the same analysis to the SNR observations measured in the *Roof* location we obtain a qualitatively not very different result, Fig. 10, although it can be observed that multipath in the *Roof* location is higher than in the *Field* location, especially for low elevations, and therefore *Field* location should be preferred for the determination of coefficients of the multipath S estimator.

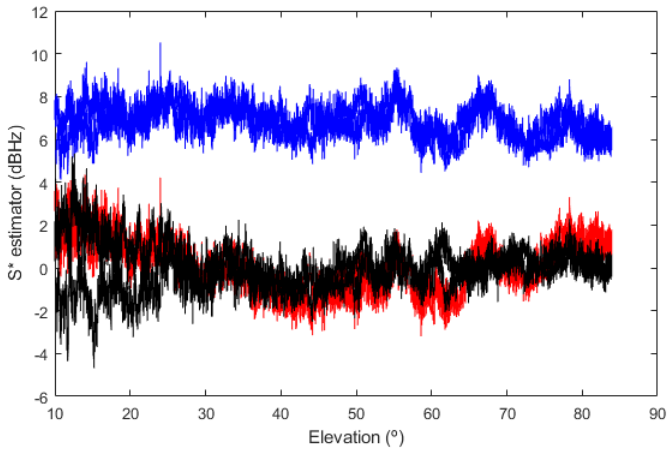

Figure 10. *Roof* location. Values for different types of the S^* estimator, Eq. (5) in terms of the elevation angle (θ): in black the complete version $S^* = S_1 - 0.4307S_2 - 0.5917S_5 - 1.3594\cos\theta$, in red the two-frequency version $S^* = S_1 - 1.0851S_2 - 8.4233\cos\theta$, in blue the simplified two-frequency version $S^* = S_1 - S_2 - \cos\theta$.

At any rate, this is the result we could expect for *Roof* location: a bit more multipath due to reflections in nearby surfaces and considerably similar α, β and γ values.

In the *Track* location we expect many more observations affected by multipath. The corresponding SNR values should not be used to determine the S^* estimator, which has to be build from (mostly) multipath-free observations. Having said that, we can also compute the S^* estimator only for the sake of illustration, Fig. 11.

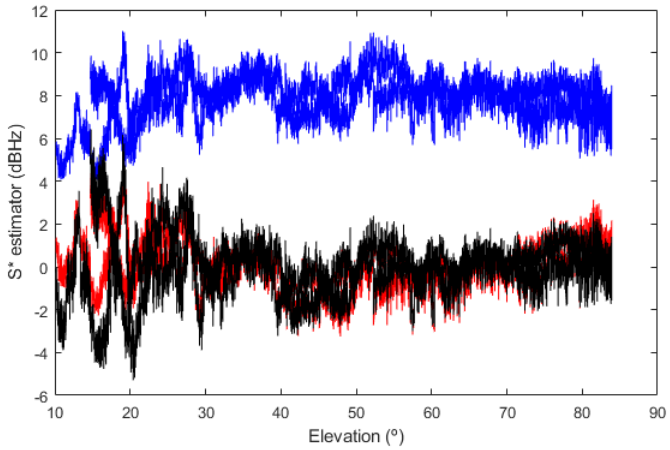

Figure 11. *Track* location. Values for different types of the S^* estimator, Eq. (5) in terms of the elevation angle (θ): in black the complete version $S^* = S_1 - 0.7252S_2 - 0.3471S_5 - 4.2531\cos\theta$, in red the two-frequency version $S^* = S_1 - 1.1203S_2 - 8.2696\cos\theta$, in blue the simplified two-frequency version $S^* = S_1 - S_2 - \cos\theta$.

In the *Track* location multipath is considerably higher at some points so that minimization of Eq. (5) does not behave so well. Indeed the significantly different from zero mean value and relatively high standard deviation (μ = 0.0116 and σ = 1.3791 for the complete version of the S^* estimator) are indicative of the existence of many undesired errors, i.e. observations affected by multipath. Further, very different values are obtained for α, β and γ compared to those in the other two locations for the case of three frequencies, although α and γ values are relatively similar in the case of two frequencies.

Please note that multipath detection in the *Track* location will not be eventually decided by using Fig. 11, but by means of the corresponding S^* values (not depicted here) obtained using the α, β and γ values as determined for a low multipath environment (*Roof* or, better, *Field*).

In theory, an individual determination of the optimal coefficients of the S^* estimator is required for every GNSS satellite. However it is worth mentioning that some similarities are found for satellites of the same constellation, especially for the S^* estimator based on two frequencies so that a general expression for every constellation could also be practical :

- In GPS satellites, the optimal estimator can be computed as

$$S^* = S_1 - 1.085S_2 - 8.5cos(\theta) \quad (7)$$

with α typically varying in a range of ±0.02 and γ in a range of ±1.5.

- In Galileo satellites, the optimal estimator can be computed as

$$S^* = S_1 - 0.85S_2 + 1.1cos(\theta) \quad (8)$$

with α typically varying in a range of ±0.02 and γ in a range of ±1.2.

- In GLONASS satellites, the optimal estimator can be computed as

$$S^* = S_1 + \alpha S_2 + \gamma cos(\theta) \quad (9)$$

with α typically varying ±0.01 from the following linear function based on the frequency number FN (1, 2, etc.)

$$\alpha = 0.0109FN - 1.1142 \quad (10)$$

and γ typically varying in a range of ±0.2 from the following quadratic function:

$$\gamma = 0.0549FN^2 - 1.5916FN + 9.8530 \quad (11)$$

It is not surprising to find a linear relationship between the different optimal α values due to the frequency division of GLONASS satellites, which is generated following a linear function. However, the reason for the second-degree polynomial that γ values follow is currently unknown.

Finally, we obtain the results of applying both the estimator S using reference functions, Eq. (3), along with the multipath detection threshold, Eq. (4), as well as the estimator using the optimal combination S^*, Eq. (5). The observations detected as free from multipath and affected by multipath as observed from the *Track* location are shown for the different GNSS signals in Fig. 12 for universal calibration and Fig. 13 for individual calibrations, both in the case of three carrier phases, and in Fig. 14 for universal calibration and Fig. 15 for individual calibrations, both in the case of two carrier phases. An elevation mask of 25 degrees has been set for all computations. It is worth mentioning that satellites G05 and G06 symultaneously show some sudden jumps in their L_2-SNR values for all observing locations (Field, Roof and Track), at 4:10 for G05 and 5:10 for G06, which may have no correlation with reflections or obstructions at the observing locations. Being their utility for detection more than questionable, these satellites have been excluded from the present example.

Please also note that some satellites do not broadcast signals in three frequencies but only in two (for instance, satellites G11 and G14); therefore, they cannot be used in the three-frequency approach.

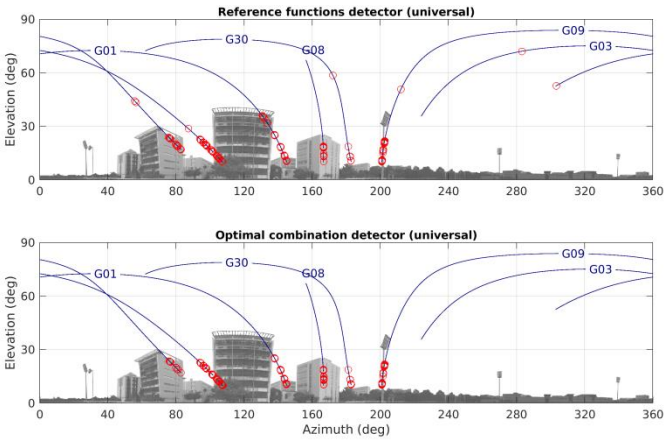

Figure 12. *Track* location. Free from multipath (in blue) or affected by multipath (red circles) observations for the S estimator, Eq. (3), in the upper panel, and the S^* estimator, Eq. (5), in the lower panel, using a universal calibration and three frequencies.

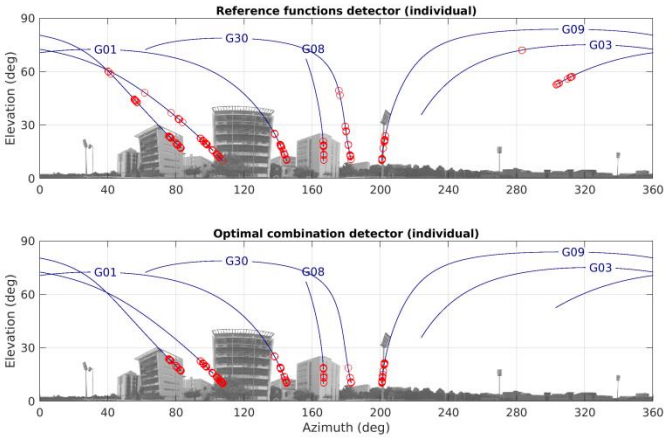

Figure 13. *Track* location. Free from multipath (in blue) or affected by multipath (red circles) observations for the S estimator, Eq. (3), in the upper panel, and the S^* estimator, Eq. (5), in the lower panel, using individual calibrations and three frequencies.

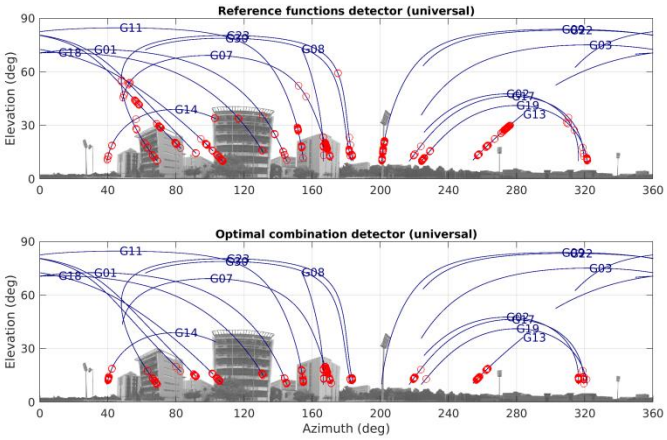

Figure 14. *Track* location. Free from multipath (in blue) or affected by multipath (red circles) observations for the S estimator, Eq. (3), in the upper panel, and the S^* estimator, Eq. (5), in the lower panel, using a universal calibration and two frequencies.

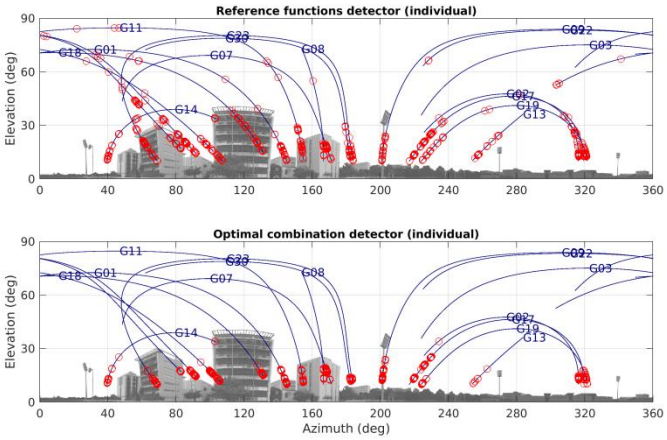

Figure 15. *Track* location. Free from multipath (in blue) or affected by multipath (red circles) observations for the S estimator, Eq. (3), in the upper

panel, and the S^* estimator, Eq. (5), in the lower panel, using individual calibrations and two frequencies.

We see that the estimator using the optimal combination of SNR values, S^* estimator, flags in general less observations as being affected by multipath. This is especially remarkable for the observations high over the horizon.

With both estimators, we also obtain some mixed results for the observations where the satellites are behind the building. At any rate, these results seem much more consistent than the results obtained by simple decision trees.

We show now the results of using the decision tree in [18, Fig. 10] for determining line-of-sight and non-line-of-sight observations in the *Track* location. We can see in the following Figs. 16 and 17 that this simple approach does not produce correct results, since it inconsistently yields line-of-sight and non-line-of-sight results for the different observations.

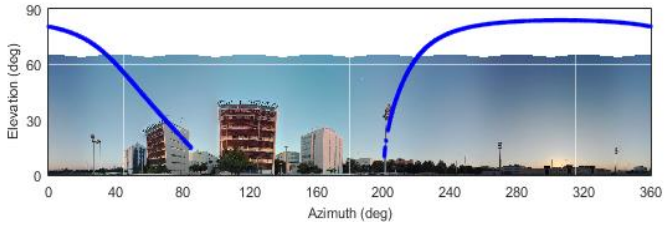

Figure 16. *Track* location. Line-of-sight observations according to the decision tree in [18, Fig. 10].

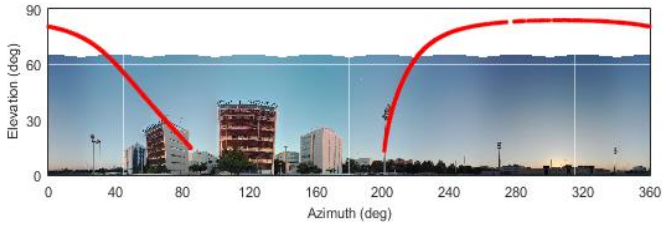

Figure 17. *Track* location. Non-line-of-sight observations according to the decision tree in [18, Fig. 10].

5. Conclusion

We have discussed several issues in the practical application of the multipath detection estimator by Strode and Groves based on the use of reference functions not only to GPS as in the original contribution [14], but also to GLONASS and Galileo constellations. In particular, we have shown the different shapes of the reference or calibration functions for every constellation and explored the possibility of using a universal calibration function for all satellites belonging to the same constellation. We observed a good agreement among the different callibration functions for the different GPS satellites and, in consequence, we were able to obtain a universal reference function to successfully model GPS SNR differences. This function resulted to be strongly dependent on satellite elevation. Also good resulted the consistency among all calibration functions for the different Galileo satellites, so that we could obtain a universal reference function to successfully model Galileo SNR differences, which, contrary to the case of GPS, happens to be fairly independent of elevation. No universal function was defined for GLONASS satellites due to the observed inconsistency among individual reference functions.

In addition, we have presented and alternative estimator for multipath detection based on the optimal combination of SNR values that seems to perform more consistenly than the estimator based on reference functions. Studying this optimal combination estimator for the cases of two and three carrier frequencies we concluded that the two-frequency estimator performs almost as well as the three-frequency version and it has a lower variability among the different satellites of the same constellation, so that handy general expressions of the optimal combination estimator to use for each constellation (GPS, Galileo and GLONASS) can be used.

We also observed that correction of antenna pattern gains did not significantly change results in any of the methods.

Finally, we also analyzed the use of a previously proposed simple decision tree, which failed to provide reasonable results in our experiments.

The application of the methods to BeiDou constellation has not been dealt with in this research. It remains, therefore, as an open question for future reseach, as well as the application of the methods to other environments and requirements, e.g. urban canyons (in the field of navigation), submillimetric length determination in baselines of reference (in the field of metrology), and application to local ties in fundamental stations (in the field of geodesy).

Acknowledgements

The authors are sincerely thankful to the editor and three anonymous referees for their comments and suggestions, which helped to considerably improve the manuscript.

References

[1] Teunissen P J G and Montenbruck O 2017 *Handbook of Global Navigation Systems* (Cham, Switzerland: Springer International Publishing)

[2] Irsigler M 2008 *Multipath Propagation, Mitigation and Monitoring in the Light of Galileo and the Modernized GPS* (Universität der Bundeswehr München, Germany: PhD Thesis)

[3] Wanninger L and May M 2000 Carrier Phase Multipath Calibration of GPS Reference Stations *Proc. ION GPS 2000* pp 132–44

[4] Baselga S, García-Asenjo L and Garrigues P 2014 Submillimetric GPS distance measurement over short baselines: noise mitigation by global robust estimation *Meas. Sci. Technol.* **25** (105004) 6 pp

[5] Groves P D, Jiang Z, Skelton B, Cross P A, Lau L, Adane Y and Kale I 2010 Novel Multipath Mitigation Methods using a Dual-polarization Antenna *23rd International Technical Meeting of the Satellite Division of the Institute of Navigation, ION GNSS* pp 2010.1.140–51
[6] Phan Q H, Tan S L and McLoughlin I 2013 GPS multipath mitigation: a nonlinear regression approach *GPS Solut.* **17** 371–80
[7] Tatarnikov D and Astakhov A 2014 Approaching Millimeter Accuracy of GNSS Positioning in Real Time with Large Impedance Ground Plane Antennas *Proc. Intl. Tech. Meeting of ION* pp 844–8
[8] Mekik C and Can O 2010 An investigation on multipath errors in real time kinematic GPS method *Sci. Res. Essays* **5** 2186–200
[9] Baselga S and García-Asenjo L 2008 Multipath Mitigation by Global Robust Estimation *J. Navig.* **61** 385–92
[10] Zhang Z, Li B, Gao Y and Shen, Y 2019 Real-time carrier phase multipath detection based on dual-frequency C/N0 data *GPS Solut.* **20** 399–412
[11] Dong D, Wang M, Chen W, Zeng Z, Song L, Zhang Q, Cai M, Cheng Y and Lv J 2016 Mitigation of multipath effect in GNSS short baseline positioning by the multipath hemispherical map *J. Geod.* **90** 255–62
[12] Fuhrmann T, Luo X, Knöpfler A and Mayer M 2015 Generating statistically robust multipath stacking maps using congruent cells *GPS Solut.* **19** 83–92
[13] Ye S, Chen D, Liu Y, Jiang P, Tang W and Xia P 2015 Carrier phase multipath mitigation for BeiDou navigation satellite system *GPS Solut.* **19** 545–57
[14] Strode P R R and Groves P D 2016 GNSS multipath detection using three-frequency signal-to-noise measurements *GPS Solut.* **20** 399–412
[15] Špánik P and Hefty J 2017 Multipath detection with the combination of SNR measurements – Example from urban environment *Geodesy and Cartography* **66** 305–15
[16] Lau L and Cross P 2006 A New Signal-to-Noise-Ratio Based Stochastic Model for GNSS High-Precision Carrier Phase Data Processing Algorithms in the Presence of Multipath Errors *ION GNSS* pp 276–85
[17] Rost C and Lambert W 2009 Carrier phase multipath mitigation based on GNSS signal quality measurements *Journal of Applied Geodesy* **3** 1–8
[18] Yozevitch R, Ben Moshe B and Weissman A 2016 *Navigation* **63** 429–42
[19] GLONASS ICD 2008 *Navigational Radiosignal in Bands L1, L2* (Edition 5.1) (Moscow, Russia: Russian Institute of Space Device Engineering).